Biochimica et Biophysica Acta, 545 (1979) 265—284

BBA 47605

CHARGE RECOMBINATION IN PHOTOSYSTEM I AT LOW TEMPERATURES

KINETICS OF ELECTRON TUNNELING *

BACON KE [a,*], SANDOR DEMETER [a,**], K.I. ZAMARAEV [b,***] and R.F. KHAIRUTDINOV [b]

[a] *Charles F. Kettering Research Laboratory, Yellow Springs, OH 45387 (U.S.A.), and*
[b] *Institute of Chemical Physics, U.S.S.R. Academy of Sciences, Moscow (U.S.S.R.)*

(Received May 8th, 1978)

Key words: Photosystem II; Electron tunneling; Charge recombination; P-700 photo-oxidation; (Kinetics)

Summary

Absorption changes accompanying light-induced *P*-700 oxidation and the decay of $P\text{-}700^+$ in the dark were measured in the temperature range 294—5 K over a broad time scale (three to four orders of magnitude). Two qualitatively different types of kinetics for the dark decay of $P\text{-}700^+$ were observed. In the 294—240-K region, a usual exponential kinetics is observed with the rate constant $k = 1 \cdot 10^{10} \cdot \exp(-16\,000/RT)\ s^{-1}$, with R in cal/mol per degree. Below 220 K, a rather unusual logarithmic or near-logarithmic kinetics are observed. These kinetics can be explained quantitatively if one assumes for the various ($P\text{-}700^+ \cdots X^-$) pairs a broad rectangular or near-rectangular distribution over the values of the rate constant. The following kinetic equation corresponding to this model was obtained:

$$n_t/n_0 = [\ln(k_{max}/k_{min})]^{-1} \cdot [\ln(1/k_{min}) - \ln t]$$

where n_0 and n_t are respectively the initial concentration of $P\text{-}700^+$ and its concentration at time t, and k_{max} and k_{min} the maximum and minimum values of the rate constant, respectively. The decay processes observed can be ascribed to electron tunneling. Distribution over the values of k can be accounted for by different environments or different mutual orientations of $P\text{-}700^+$ and X^-, or by different distances between them in the various reacting pairs.

The corresponding distribution function was reconstructed from the experi-

---

* Contribution No. 600 from the Charles F. Kettering Research Laboratory.

* To whom correspondence and reprint request should be addressed.
** Present address: Institute of Plant Physiology, Hungarian Academy of Sciences, Szeged, Hungary.
*** Present address: Institute of Catalysis, U.S.S.R. Academy of Sciences, Novosbirsk, U.S.S.R.

Abbreviation: TSF-I, Triton-fractionated Photosystem I subchloroplasts fragments.

mentally measured $P\text{-}700^+$-decay curves. The rate of tunneling was found to be temperature dependent. In the 160—80-K region, the temperature dependence corresponds to an activation energy of 2.9 kcal/mol. Below 80 K, new modes of $P\text{-}700^+$ decay with lower activation energy become operative. The tunneling distance for the majority of the ($P\text{-}700^+ \cdots X^-$) pairs was estimated from the EPR linewidth of $P\text{-}700^+$ to exceed 13.2 Å.

Introduction

Low-temperature photooxidation of *P*-700 was first reported by Calvin and Sogo [1] from EPR measurements, and by Müller and Witt [2] from measurements of absorption changes. Subsequent reports by various other workers (refs. 3—5, by EPR; refs. 6—9, by absorption-change measurements) led to contradictory results regarding the decay kinetics at low temperatures (see ref. 16 for a summary of earlier works). More recent works, either using EPR spectroscopy alone [10,11,18] or using both EPR and optic spectroscopies [12—17], yielded reasonably consistent results of apparent multiphasic decay kinetics at low temperatures. But a generally acceptable interpretation on the reaction mechanism has not yet been reached.

Warden et al. [10,11] examined the temperature dependence of $P\text{-}700^+$ decay by EPR spectroscopy and reported that in the temperature range 150—270 K it follows first-order kinetics, with an activation energy of 5.5 kcal/mol. Below approx. 150 K, only 10—30% of the signal was reversible (the irreversible or slowly reversible portions of the signal were pre-bleached prior to the measurements), with a decay time of 0.8 s. The "temperature-independent" decay time between 5 and 150 K was interpreted in terms of a quantum-mechanical tunneling model.

Visser et al. [13,14] and Ke et al. [15,16] made detailed EPR and optical spectroscopic measurements of the photooxidation of *P*-700 and its dark decay over a wide range of temperatures. Both groups found *P*-700 photooxidation to be partially reversible at low temperatures, and that a greater proportion of the change became irreversible with lowering temperatures. Both groups also suggested electron tunneling to be the mechanism for these low-temperature reactions. Visser et al. [13,14] attributed the different time constants associated with the decay phases below 150 K to different distances separating *P*-700 and the bound ferredoxin in the reaction centers. Ke et al. (ref. 16; see also refs. 12, 13 and 17) demonstrated the identity between the decay kinetics of $P\text{-}700^+$ monitored by EPR and optic spectroscopies and the extreme sensitivity of light-induced absorption changes at low temperatures to the intensity of the measuring light. Visser et al. [13,14], Ke et al. [15] and Bearden and Malkin [18] also found that the redox states of $P\text{-}700^+$ and of the reduced iron-sulfur protein are stoichiometrically related. Thus, the kinetic data are consistent with the suggestion that the bound iron-sulfur protein functions as the primary electron acceptor of Photosystem I.

Two electron-transfer reactions in photosynthetic bacteria at low temperatures have been suggested to take place by the tunneling mechanism: one is the oxidation of cytochrome *c* by the oxidized primary donor molecule, $P\text{-}890^+$,

in *Chromatium* [19,20], the other is the recombination of the oxidized primary donor, *P*-870$^+$, with the reduced primary acceptor, X^-, in *Rhodopseudomonas spheroides* and *Rhodospirillum rubrum* [21,22]. In the case of cytochrome oxidation, the half-time $t_{1/2}$ between 100 and 4.5 K is practically constant at 2.3 ms; in the 100—300-K region, $t_{1/2}$ decreases from 2.3 ms to 2 μs. The temperature dependence above 100 K corresponds to an activation energy of 3.3 kcal/mol; that below 100 K to less than 4 cal/mol. In the case of charge recombination in photosynthetic bacteria, the decay rate was found to be temperature independent between 1.5 and 80 K and to obey approximately first-order kinetics [21,22], but the decay time increases with increasing temperature above approx. 150 K [22]. Subsequently, theoretical models have been proposed by various other workers [23—26] to explain the observed kinetics of the cytochrome oxidation reaction.

The present paper reports a quantitative analysis of the kinetics of charge recombination in Photosystem I reaction centers measured by absorption changes in the temperature range from 294 to 5 K over a time span of three to four orders of magnitude. The analysis indicates the charge recombination in Photosystem I in the 294—240-K region follows the usual exponential kinetics, with an activation energy of 16 kcal/mol. Below approx. 240—22 K, presumably that corresponding to vitrification of the sample matrix, the decay process can be ascribed to electron tunneling.

The decay process below 240 K follows a rather unusual logarithmic or near-logarithmic kinetics which can be quantitatively explained if one assumes a rectangular or near-rectangular distribution function for the distances separating the reacting species, or for some other parameters of which the rate constant is an exponential function.

The kinetics of electron tunneling is temperature dependent. In the 160—80-K region, the temperature dependence corresponds to an activation energy of 2.9 kcal/mol and can be ascribed to a tunnel electron transfer involving an excited state of the (P-700$^+$ ··· X^-) assemblies. Below 80 K, new modes of P-700$^+$ decay with lower activation energy seem to become operative. In the 180—140-K region, the characteristic time of electron tunneling decreases with decreasing temperature. Just as in the case of photosynthetic bacteria, such an effect can be ascribed to some conformational transition in the chloroplast membrane bringing P-700$^+$ and iron-sulfur protein further apart as temperature increases.

Experimental

Triton-fractionated Photosystem I subchloroplast fragments (TSF-I) prepared according to ref. 27 were used throughout the experiments. The TSF-I preparation contained one *P*-700 per 55 bulk chlorophyll molecules, and had a NADP reduction activity of 1000 μmol/mg chlorophyll per h. The TSF-I fragments were suspended in 0.1 M Tricine-NaOH, pH 8.0, containing 55% glycerol and 1 M sucrose (all referred to final concentrations). No exogenous secondary electron donors or acceptors were added. Transparent samples were obtained in this medium at all temperatures. All chemicals were of reagent grade and were used without further purifications.

For the light-induced absorption-change measurements, the sample was placed in a vucette constructed from copper frames and thin Lucite-plate windows [28]. When used in the cuvettes of 1 mm pathlength, the TSF-I sample had an absorbance of 1.5 per mm at the red absorption maximum. The metal cuvette was used in conjunction with a modified quartz dewar adapted to a helium refrigerator and associated liquid helium transfer line and temperature controller (Air Products Heli-tran System LTD-3-100) to achieve desired low temperatures [16]. For each of the measurements, which range from minutes to over 10 h, the sample temperature could be maintained to within 1 K or better. Liquid nitrogen was used as the refrigerant for temperatures above 80—90 K, and liquid helium for the lower temperatures.

The light-induced absorption changes due to *P*-700 photooxidation was monitored at 700 nm vs. 725 nm as the reference wavelength in a modified dual-wavelength spectrophotometer with a high degree of stability and provisions to eliminate the interference due to fluorescence and scattering [29]. Polychromatic blue (400—460 nm) light isolated by a Baird-Atomic interference filter with an intensity of $4.7 \cdot 10^5$ ergs/cm^2 per s was used for excitation. Due to the sensitivity of the absorption changes to the intensity of the measuring light at low temperatures [16], the measuring light was usually maintained at an intensity of approx. 2—3 ergs/cm^2 per s. The sample was illuminated for 10 s through a shutter (Vincent Assoc. model 225L4A0X5), which has an opening and closing time of about 5 ms. For each temperature, the dark decay was measured continuously for 180 s. At subsequent points in time, a recording was made for 10 s to register the new level of absorption. The measuring light was cut off from the sample at all times except during the time when recordings were made.

Results and Discussion

Kinetics of P-700$^+$ decay in the 294—240-K region

Absorption changes accompanying light-induced *P*-700 oxidation and the decay of *P*-700$^+$ in the dark were measured at temperatures ranging from ambient (294 K) to 10 K, at 10-K intervals, and also at 5 K. Two qualitatively different types of kinetics for the dark decay of *P*-700$^+$ were observed. In the 294—240-K region, the rate of the decay process is characterized by the fact that the fraction of *P*-700$^+$ disappearing within some fixed time interval decreases continuously as the temperature is lowered (Fig. 1). Within this temperature range, the dark decay of *P*-700$^+$ follows the usual exponential kinetics, as shown by the logarithmic plot in Fig. 2. The kinetics represented by these plots are consistent with the relationship $n_t = n_{t_0} \cdot \exp[-k(t - t_0)]$, where n_t and n_{t_0} are the number of *P*-700$^+$ molecules at time t and time t_0, respectively, and t_0 is a fixed moment in time and is chosen to be 12.5 s after the termination of illumination, and k is the rate constant for the decay process.

Referring to the Arrhenius equation, $k = k_0 \cdot \exp(-E_a/RT)$ or $\ln k = \ln k_0 - E_a/RT$, the activation energy, E_a, for the *P*-700$^+$ decay in the 294—240-K region can be calculated from the slope of the plot of $\ln k$ vs. $1/T$, as shown in Fig. 3. The activation energy is estimated to be $16 \cdot 10^3$ cal/mol. The pre-exponential frequency factor, k_0, has the value of $1 \cdot 10^{10}$ s^{-1}. Thus the *P*-700$^+$

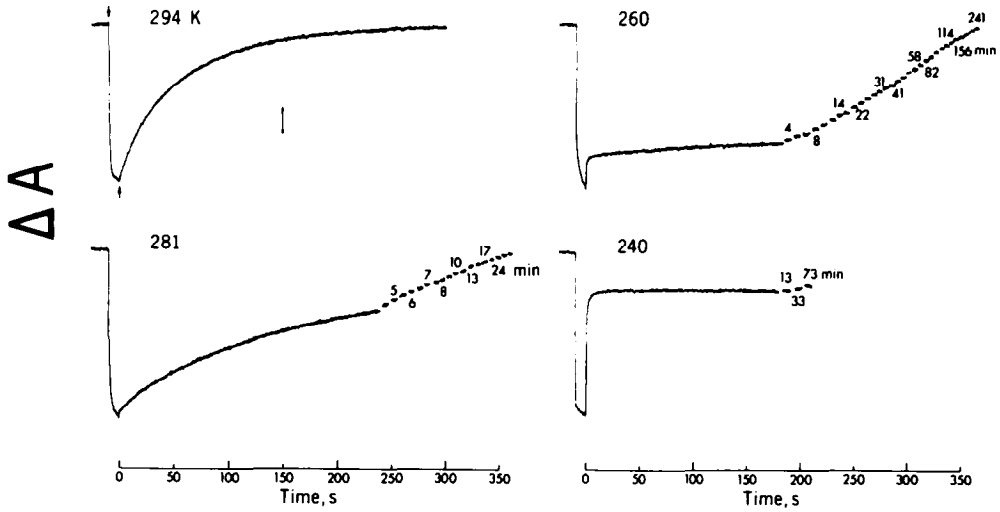

Fig. 1. Light-induced absorption changes accompanying *P*-700 photooxidation and the decay of *P*-700$^+$ in the dark in TSF-I subchloroplast fragments at 294, 281, 260 and 240 K. Sample and experimental conditions are described in detail in the text. Illumination period, 10 s. Downward arrow, light on; upward arrow, light off (shown for the 294-K trace). The vertical bar (in the 294-K trace) represents a transmission change ($\Delta T/T$) of 0.01. The bottom time scale (zero time at termination of illumination) applies only to the continuous recording of decay. At subsequent points in time, recordings were made for 10 s to register the new level of absorption. Some of the time points are indicated in the figure. The monitoring light was cut off from the sample at all times except when recordings were made.

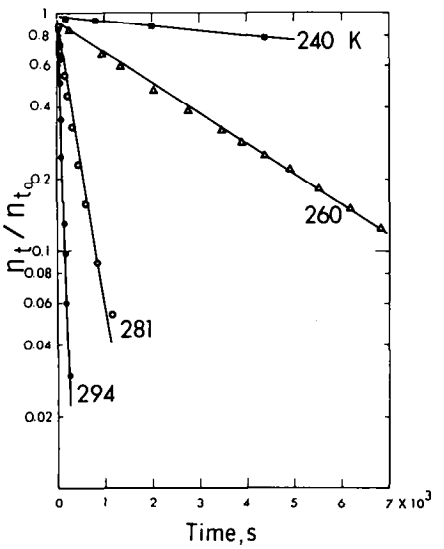

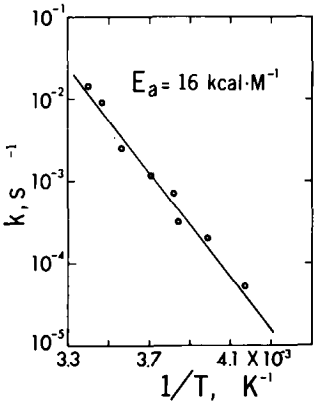

Fig. 2. Curves of *P*-700$^+$ decay plotted as $\ln(n_t/n_{t_0})$ vs. time t. Time t_0 was chosen to be 12.5 s after the termination of illumination.

Fig. 3. Dependence of the rate constant k (derived from data like those in Fig. 2) on the reciprocal temperature, $1/T$.

decay process in the 294—240-K region can be represented by the kinetic equation:

$$k = 1 \cdot 10^{10} \cdot \exp(-16 \cdot 10^3/RT)\ s^{-1}$$

with R in cal/mol per degree.

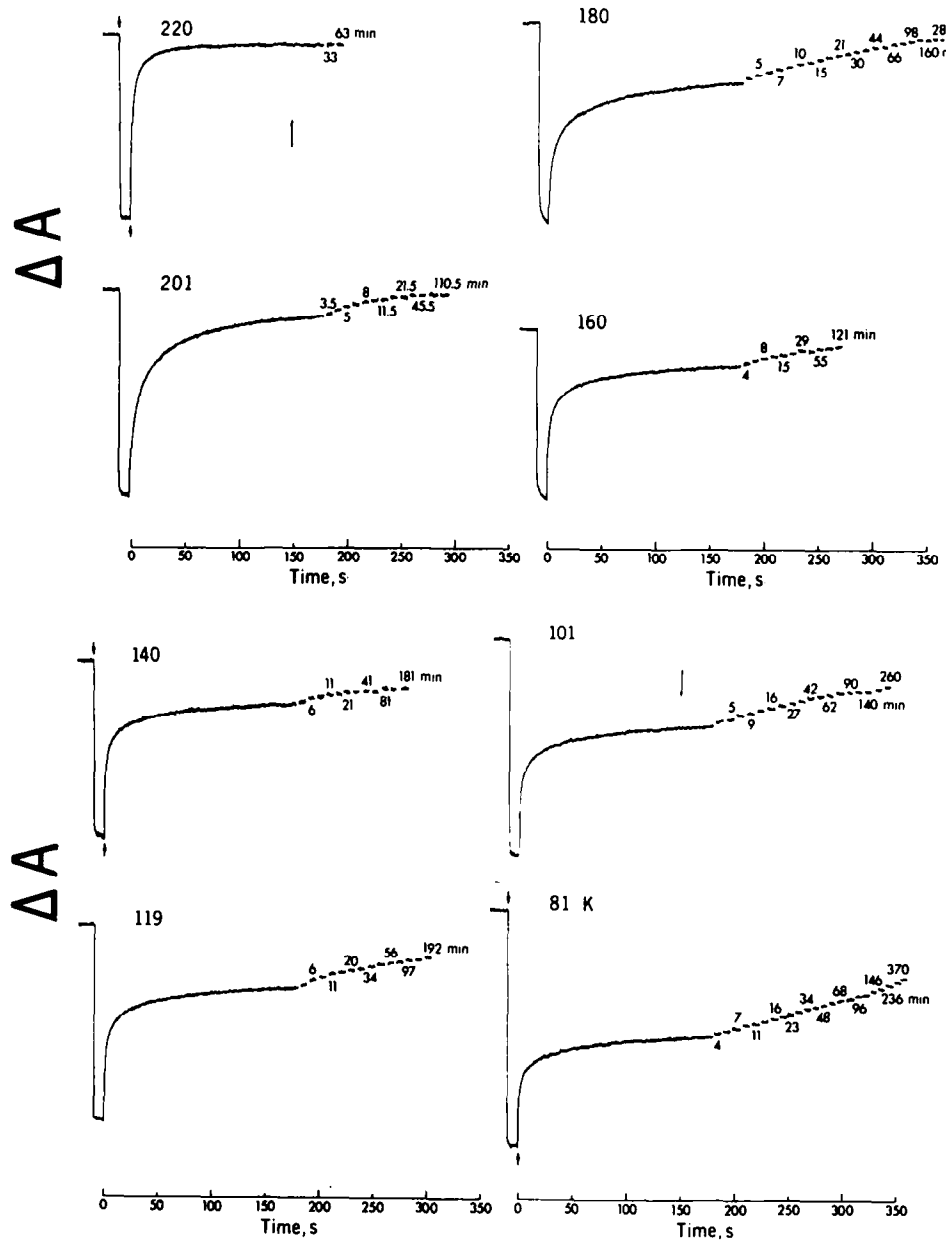

Fig. 4. Light-induced absorption changes accompanying *P*-700 photooxidation and the decay of *P*-700$^+$ in the dark in TSF-I subchloroplast fragments in the 220—80-K region. Other conditions were the same as in Fig. 1.

Kinetics of P-700$^+$ decay at temperatures below 240 K

Light-induced absorption changes due to *P*-700 photooxidation and the dark decay of *P*-700$^+$ at temperatures below 240 K are presented in Figs. 4 and 5. A rather unusual change in the overall rate of *P*-700$^+$ decay is observed in the 240—220-K and 180—140-K regions. Comparing the dark decay kinetics at 240 K (Fig. 1) and 220 K (Fig. 4), it can be seen that the overall rate of *P*-700$^+$ decay increases notably as the temperature is lowered from 240 to 220 K. For example, at 240 K, 80% of *P*-700$^+$ decayed at the end of 73 min, while at 220 K, about 96% of *P*-700$^+$ disappeared at the end of 3 min. A similar conclusion follows from comparison of the decay curves at 180 K and at 160 or 140 K. Such a change is contrary to the usual kinetic behavior of most chemical reactions on temperature dependence.

For the *P*-700$^+$ decay at temperatures below 220 K, we plot the number of *P*-700$^+$ molecules at time t, n_t vs. log t, as shown in Fig. 6. The curves have different characteristics for the regions 220—160 K, 160—180 K and 80—5 K. In the 80—5-K region, the logarithmic decay curves are linear throughout the whole time span. In the 160—80-K regions, they are linear only for the initial portions of the decay; at longer decay times, the decay rate as expressed by the change of n_t with respect to the logarithm of time is lower than at shorter times. In the 220—160-K region, deviation from linearity is observed throughout the whole time span. Furthermore, the initial slope of the decay curves remains practically constant in the 160—80-K region and becomes temperature dependent below 80 K and above 160 K.

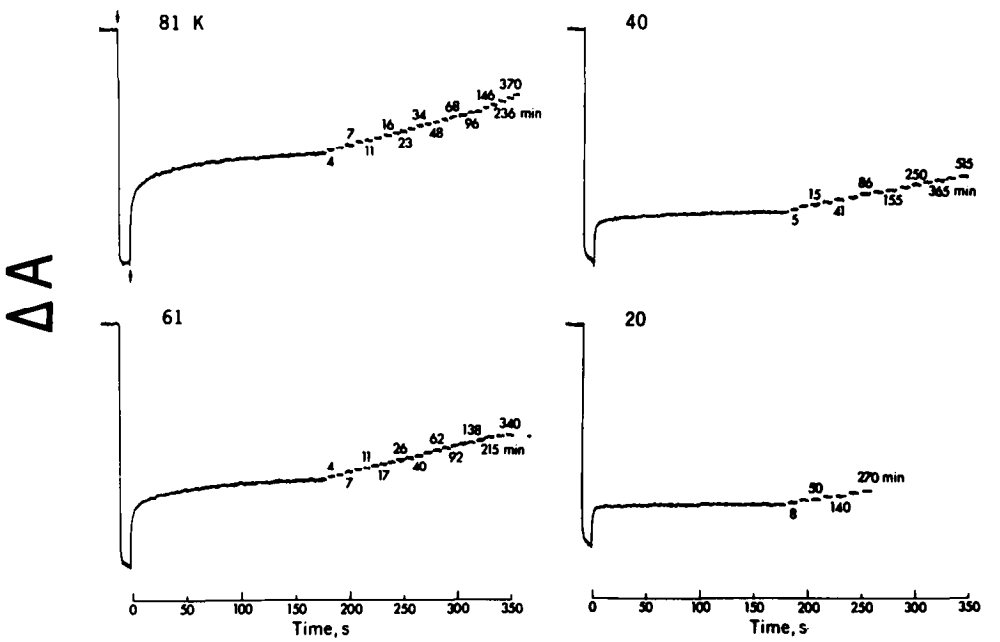

Fig. 5. Light-induced absorption changes accompanying *P*-700 photooxidation and the decay of *P*-700$^+$ in the dark in TSF-I subchloroplast fragments at 81, 61, 40 and 20 K. Other conditions were the same as in Fig. 1.

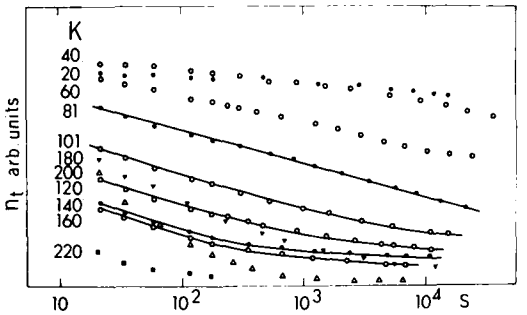

Fig. 6. Curves of $P\text{-}700^+$ decay plotted as n_t vs. ln t for the 220—20-K region. Time is calculated from the point of termination of illumination. For temperatures at 80—160 K, the solid lines are calculated from Eqn. 6 and the near-rectangular distribution functions of Fig. 10.

Electron tunneling in the solid-phase reaction

The switch-over of the overall reaction rate of $P\text{-}700^+$ decay in the 240—220-K region most likely corresponds to vitrification of the sample. The switch-over in the kinetic behavior of the $P\text{-}700^+$ decay at the moment of vitrification may be explained as arising from recombination of $P\text{-}700^+$ with two "types" of primary acceptors (X and X') *, namely

$$P\,700^+ + X^- \rightarrow P\,700 + X \qquad (1)$$

which is predominant above 240 K and has an activation energy, E_a, of $16 \cdot 10^3$ cal/mol, and

$$P\,700^+ + X'^- \rightarrow P\,700 + X' \qquad (2)$$

which is predominant below 220 K and has a lower activation energy, E'_a. In the 240—220-K region, both types of reactions occur simultaneously. The difference in the "types" of acceptor may either be one in the bulk chemical composition or one in the structural arrangements or conformational states around one type of $P\text{-}700^+$-acceptor pairs caused by vitrification. As E_a is greater than E'_a at low temperatures, reaction 1 is slower than reaction 2. This explains why a switch from acceptor X' to X as the temperature is raised from 220 to 240 K is followed by a decrease in the overall rate of $P\text{-}700^+$ decay.

The exponential character of the $P\text{-}700^+$ decay kinetics at temperatures above approx. 240 K clearly indicates that the recombination of $P\text{-}700^+$ with the reduced acceptor X^- is the only process responsible for the observed decay. No intermediate steps are observed for this process for the time scale studied.

The fact that the reaction is observed at very low temperatures when diffusion of $P\text{-}700^+$ and X'^- in chloroplasts seems impossible indicates that reaction 2 takes place by the mechanism of long-range electron tunneling.

It is known that there are at least two membrane-bound iron-sulfur proteins in the photosystem I reaction center which can be photochemically reduced

* Recent reductive titrations of the Photosystem I subchloroplast particles monitored by light-induced EPR and absorption changes at 15 K [30—32] confirmed and extended the suggestion [33,34] that an intermediary electron acceptor "I" may precede the stable primary electron acceptor X. The time of electron transfer from the intermediary to the stable primary electron acceptor is unknown but presumed to be very fast. For this reason, it is omitted in the formulation in reactions 1 and 2.

[35—37]. Available evidence from the parallel decay kinetics of $P\text{-}700^+$ and the iron-sulfur protein at low temperatures indicates that the bound iron-sulfur protein with a midpoint potential of —530 mV apparently functions as the stable primary acceptor, at least at very low temperatures [13,15,18]. Results from various experiments on the attenuation of photochemical formation of $P\text{-}700^+$ by reductive titration and monitored by optic and EPR spectroscopy are also consistent with the above notion [30—32]. Thus, for our present discussion, we assume that the switch-over in the kinetic behavior near 220—240 K is the result of structural or conformational changes in the pair consisting of P-700 and bound iron-sulfur protein with a mid-point potential of —530 mV as a result of vitrification. Very little is known at present about the second bound iron-sulfur protein which has a more negative redox potential. In the absence of any precise information on the dependence of its photochemical transformations on temperature [35—37], the possibility of the switch-over in decay kinetics in the 240—220-K region as involving two chemically different iron-sulfur proteins cannot be excluded completely at this time.

The rectangular distribution function

The logarithmic or near-logarithmic decay for the charge recombination in Photosystem I is characteristic for a process with a rectangular or near-rectangular distribution of the various pairs of reacting species ($P\text{-}700^+ \cdots X^-$), over the value of some distribution parameter α, of which the rate constant is an exponential function [38]:

$$k = k^{(0)} \cdot \exp(-\alpha) \tag{3}$$

where $k^{(0)}$ is assumed to be the same for all the reacting species, while α differs for the various reacting pairs. The distribution may be that over a number of parameters. For instance, it may be a distribution over the value of activation energy, E'_a. In this case, $\alpha = E'_a/RT$. However, for $P\text{-}700^+$ decay, at least in the 160—80-K region, a distribution over the value of activation energy cannot be responsible for the observed kinetics, as the slopes of the decay curves are independent of temperature (see Fig. 6; also cf. analysis below).

Note that at moment t those reacting pairs ($P\text{-}700^+ \cdots X^-$) will predominantly recombine for which the condition $k \cdot t \approx 1$, that is, $k^{(0)} \cdot t \cdot \exp(-\alpha) \approx 1$, or

$$\alpha \approx \ln(k^{(0)} \cdot t) \tag{4}$$

is fulfilled. Since the exponent is a very sharp function, practically all the pairs with $\alpha < \ln(k^{(0)} \cdot t)$ must disappear by moment t, while all the pairs with $\alpha > \ln(k^{(0)} \cdot t)$ must remain practically unreacted.

In the $P\text{-}700^+$ decay reaction, the overall change in the concentration of $P\text{-}700^+$, n_t, may be related to the rate constant, k, or the distribution parameter, α, by the following equations:

$$n_t = \int_0^\infty n_0(k) \cdot \exp(-kt)\, dk \tag{5}$$

or

$$n_t = \int_0^\infty n_0(\alpha) \cdot \exp[-k(\alpha)t]d\alpha$$

$$= \int_0^\infty n_0(\alpha) \cdot \exp[-k^{(0)} \cdot t \cdot \exp(-\alpha)]\, d\alpha \qquad (6)$$

where $\int_0^\infty n_0(k)dk = n_0$, $\int_0^\infty n_0(\alpha)d\alpha = n_0$, n_0 being the total initial concentration of the reacting pairs, $n_0(k)dk$ and $n_0(\alpha)d\alpha$ are the concentrations of the reacting pairs which have at the initial moment, $t = 0$, the value of the rate constant k from k to $k + dk$ and that of the distribution parameter α from α to $\alpha + d\alpha$, respectively. Note that Eqns. 5 and 6 are valid not only for the rectangular distribution but also for any other types of distribution over the values of k or α.

For the particular case of rectangular distribution over α and for such values of t that satisfy the condition

$$1/k^{(0)} \cdot \exp(-\alpha_{max}) >> t >> 1/k^{(0)} \cdot \exp(-\alpha_{min}) \qquad (7)\ *$$

one eventually arrives at the equation (see Appendix for its derivation)

$$n_t/n_0 = (\alpha_{max} - \alpha_{min})^{-1} \cdot [\alpha_{max} - \ln(k^{(0)} \cdot t)] \qquad (8)$$

It follows from Eqn. 3 that $\alpha_{max} = \ln(k^{(0)}/k_{min})$ and $\alpha_{min} = \ln(k^{(0)}/k_{max})$, where k_{min} and k_{max} are respectively, the minimum and maximum values of the rate constant. With these expressions, eqn. 8 may be transformed to

$$n_t/n_0 = [\ln(k_{max}/k_{min})]^{-1} \cdot [\ln(1/k_{min}) - \ln t] \qquad (8a)$$

Thus, for the rectangular distribution of $P\text{-}700^+$ concentration, n_t is indeed a logarithmic function of time t provided the condition in Eqn. 7 is fulfilled. For shorter and longer times, i.e. for $t \lesssim 1/k^{(0)} \cdot \exp(-\alpha_{min})$ or for $t \gtrsim 1/k^{(0)} \cdot \exp(-\alpha_{max})$, Eqn. 8 becomes incorrect and thus the relationship between n_t and ln t can deviate from linearity. This seems to be the case for $P\text{-}700^+$ decay in the 220—100-K region shown in Fig. 6. It is further seen from Eqn. 8 that in the 160—80-K region a distribution over the activation energy was not responsible for the observed kinetics, as otherwise the slope of the initial logarithmic portions of the decay curves, i.e. $1/(\alpha_{max} - \alpha_{min})$ $[=RT/(E'_{a,max} - E'_{a,min})]$, would be temperature dependent. As seen from Fig. 6, this is not the case.

It also follows from Eqns. 8 and 8a that it is the span of α, or the variation in the rate constant, k, rather than the absolute values of these parameters that determine the slope of the logarithmic decay curves: the broader the distribution over α or over k, the smaller the slope.

In the long-range electron-transfer reaction (electron tunneling), the driving force is a very weak but finite interaction between the reacting species. The energy of this interaction is protportional to the overlap of the wave functions of the reacting species. Since these wave functions decay approximately exponentially with distance, r, their overlap and probability of tunneling also decrease with the distance between the interacting species in an exponential manner. Thus, the rate constant for the long-range electron tunneling process can be represented by

$$k = \nu \cdot \exp(-2r/a) \qquad (9)$$

where ν is the so-called frequency factor **, a is the parameter which charac-

---

* Note that $1/k^{(0)} \cdot \exp(-\alpha_{max})$ and $1/k^{(0)} \cdot \exp(-\alpha_{min})$ are, respectively, the decay times for pairs with the maximum and minimum possible values of α or, correspondingly, with the minimum and maximum values of the rate constant k.

** In the simplest model of tunneling proposed originally by Gamow [39], ν is the frequency of electron collisions with the barrier. However, recent, more sophisticated treatment showed that this parameter is a rather complicated one and it can be temperature dependent [24,25,40].

terizes the dimunition of the overlap of wave functions of $P\text{-}700^+$ and X'^- with distance [38,40]. Thus the rectangular distribution may be that over r, a, or probably over some other parameters of which ν is an exponential function. The distribution over ν or a could perhaps arise from different mutual orientations or different environments of the reacting species. It is quite likely that in solids at low temperatures, the differences in mutual orientations, in the environments, or in the distances separating the reacting species, are not averaged out by their movement in the subchloroplast fragments.

Activation energy for electron tunneling during P-700$^+$ decay in the 160–80-K region

Combining the values of n_t and n_{t_0} given by Eqn. 8 for time t and for some fixed moment of time t_0, one obtains

$$n_t/n_{t0} = 1 - [\alpha_{max} - \ln(k^{(0)} \cdot t_0)]^{-1} \cdot \ln(t/t_0) \quad (10)$$

The activation energy E'_a for the electron-tunneling process in the 160—80-K region may be estimated with the help of this equation. First, the temperature dependence of the slope $[\alpha_{max} - \ln(k^{(0)} \cdot t_0)]^{-1}$ in Eqn. 10 can be obtained from the plot of n_t/n_{t_0} vs. $\ln(t/t_0)$ shown in Fig. 7. As the results in Fig. 6 show, all the reacting pairs in the 160—80-K region recombine with the same E'_a, i.e. there is no distribution over this parameter. Thus, in the Arrhenius equation for the rate constant, $k = k_0 \cdot \exp(-E'_a/RT)$, it is the pre-exponential factor k_0 and not the exponential factor $\exp(-E'_a/RT)$ that is different for different reacting pairs. Since the term $\exp(-E'_a/RT)$ is the same for all the reacting species, one can incorporate it into the constant parameter $k^{(0)}$ in Eqn. 3 and represent the latter as $k^{(0)} = k_0^{(0)} \cdot \exp(-E'_a/RT)$, where $k_0^{(0)}$, being part of the pre-exponential factor k_0 (from relations $k = k^{(0)} \cdot \exp(-\alpha)$, $k = k_0 \cdot \exp(-E'_a/RT)$ and $k^{(0)} = k_0^{(0)} \cdot \exp(-E'_a/RT)$, it follows that $k_0 = k_0^{(0)} \cdot \exp(-\alpha)$), does not depend on temperature, or is only a weak (i.e. non-exponen-

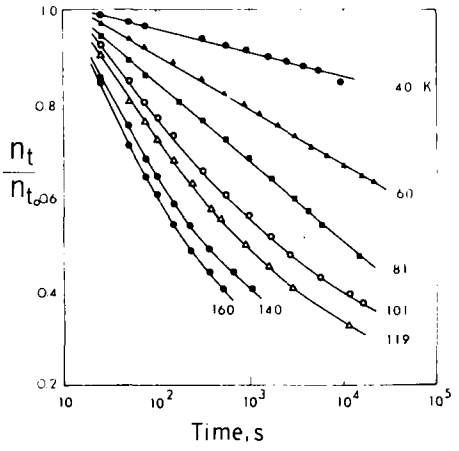

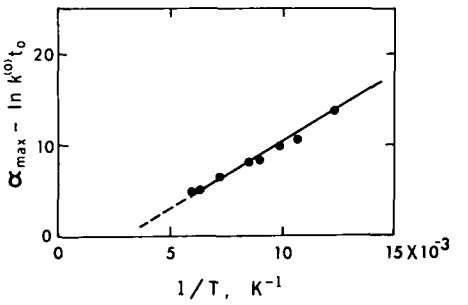

Fig. 7. Curves of $P\text{-}700^+$ decay plotted as n_t/n_{t_0} vs. $\ln(t/t_0)$ for the 160—40-K region. Time t_0 was chosen to be 12.5 s after the termination of illumination.

Fig. 8. Dependence of $\alpha_{max} - \ln(k^{(0)} \cdot t_0)$ (calculated from the initial slope of decay curves in Fig. 7) on the reciprocal temperature, $1/T$.

tial) function of it. Thus, the reciprocal of the slope in Eqn. 10 can be transformed to:

$$\alpha_{max} - \ln(k^{(0)} \cdot t_0) = \alpha_{max} - \ln(k_0^{(0)} \cdot t_0) + E'_a/RT \quad (11)$$

As shown in Fig. 8, $\alpha_{max} - \ln(k^{(0)} \cdot t_0)$, which is the reciprocal value of the slope obtained from Fig. 7, is indeed a linear function of $1/T$. From the slope of this plot, and with the help of Eqn. 11, the value of activation energy for the tunneling process in the 160—80-K region was calculated to be $2.9 \cdot 10^3$ cal/mol.

At temperatures below 80 K or above 160 K (up to 200 K) the initial slope of the kinetic curves becomes temperature dependent; it decreases continuously with decreasing temperature (cf. Fig. 6). This fact seems to indicate that outside the 160—80-K region the distribution over the values of the rate constant k becomes continuously broader with decreasing temperature.

Temperature dependence of electron-tunneling kinetics may be visualized as follows: when electron tunneling takes place from the ground state of the donor-acceptor pair, then its rate can be temperature independent. But, sometimes tunneling by an alternate mechanism may be faster. For instance, the donor species may be brought first to some excited vibrational level and then tunneling occurs from this level. Another possibility may be tunneling from some favorable position which can be achieved by a hindered rotation of the donor or the acceptor species. Since vibrational excitation or hindered rotation require activation, the rate constant of such a tunnel process must be temperature dependent, i.e.

$$k = [\nu \cdot \exp(-2r/a)] \cdot \exp(-E'_a/RT) \quad (12)$$

The charge recombination involving $P\text{-}700^+$ and X'^- in the 220—80-K region seems to be an example of such a process.

It may be noted that the procedure for calculating the activation energy from the decay curves obeying Eqns. 10 and 11 is substantially different from the usually used procedure for calculating this parameter from the slope of the relation between $\ln \tau$ (where τ is the time at which a given fraction of $P\text{-}700^+$ has decayed) and temperature. The latter procedure is obviously correct if all the reacting species in a mono- or bimolecular chemical reaction have a single rate constant. This was not the case in our present kinetics. To illustrate this point, the Arrhenius plots of the $P\text{-}700^+$ decay times for various extents of $P\text{-}700^+$ decay (for example, $\tau_{0.3}$ corresponds to a decay of 30% of the initial $P\text{-}700^+$ level) are presented in Fig. 9. It can be seen that the dependence of $\ln \tau$ on $1/T$ has a complicated character, which cannot be described by a simple linear function. These plots show three regions of temperature dependence for $\ln \tau$: (a) in the 220—180-K region, $\ln \tau$ decreases with increasing temperature: (b) in the 180—140-K region, $\ln \tau$ increases with increasing temperature, which would formally mean a negative value for the activation energy; and (c) at temperatures below 140 K, $\ln \tau$ again decreases with increasing temperature. As seen from the activation energy values estimated in this manner and shown in the legend of Fig. 9, the activation energy determined from the Arrhenius plots for temperatures below 140 K and above 180 K depends on the extent of $P\text{-}700^+$ decay.

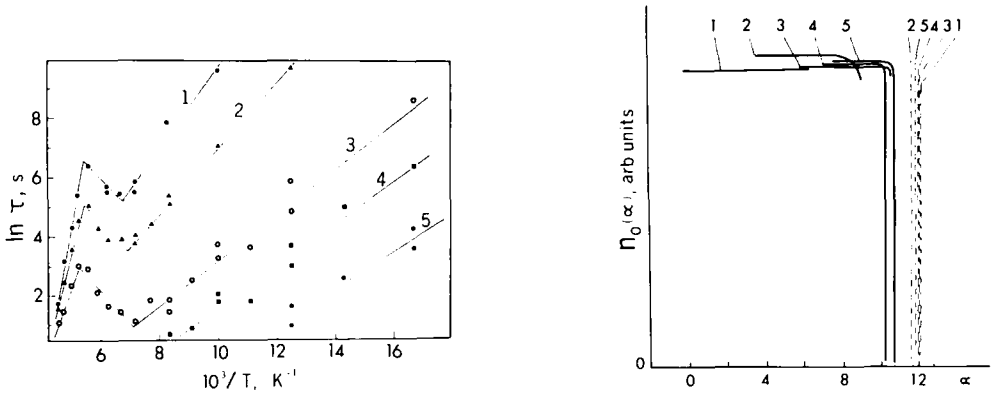

Fig. 9. Dependence of ln τ (derived from the decay curves in Figs. 1, 4 and 5) on the reciprocal temperature, $1/T$. Curves 1—5 are plotted for 80 (represented by $\tau_{0.8}$), 70, 50, 40 and 30% decay, respectively, from the original $P\text{-}700^+$ level. The activation energy estimated from these plots are: (1) $\tau_{0.8}$, E_a = 2.35 kcal/mol; (2) $\tau_{0.7}$, E_a = 2.25 kcal/mol; (3) $\tau_{0.5}$, E_a = 1.55 kcal/mol; (4) $\tau_{0.4}$, E_a = 1.40 kcal/mol; and (5) $\tau_{0.3}$, E_a = 1.25 kcal/mol.

Fig. 10. Segments of the distribution function reconstructed from the decay curves of Fig. 6, using Eqns. 6 and 13 (solid lines) and the edges of the ideal rectangular distribution (dashed lines) at various temperatures: 1, 80 K; 2, 101 K; 3, 120 K; 4, 140 K; and 5, 160 K.

Reconstruction of the rectangular distribution function over the values of α

Using Eqn. 6, the distribution function over the values of α (i.e. over the values of the rate constant k) for the ($P\text{-}700^+ \cdots X'^-$) pairs may be reconstructed. In order to do this, the theoretical decay curves were calculated for several types of $n_0(\alpha)$ functions by means of numerical integration of Eqn. 6 and then the function which provided the fit between the theoretical and the experimental decay curves was selected. Fig. 10 presents the distribution function which best fit the observed $P\text{-}700^+$ decay kinetics of Fig. 6.

In fact, we used the procedure of consecutive approximation to find these functions for each temperature. At first, simple probe functions $n_0(\alpha)$ were constructed. When constructing these probe functions, we took in mind some simple considerations mentioned above: namely, that the constancy of the decay-curve slopes in Fig. 6 implies a rectangular character of $n_0(\alpha)$, while the decrease of the slope at longer times t implies the decrease of $n_0(\alpha)$. Then these probe functions were consequently improved to provide the fit between the theoretical and the experimental decay curves.

Note that in representing the rate constant as $k = k^{(0)} \cdot \exp(-\alpha)$ (Eqn. 3), we maintained from the very beginning some ambiguity about the absolute values of α and $k^{(0)}$. Indeed one may freely choose the smallest value for α. For example, for a rectangular distribution we may assume $\alpha_{min} = 0$. Then $k^{(0)}$ will be equal to the largest rate constant possible for the process (i.e. $k^{(0)} = k_{max}$). But we may also choose any other value for α_{min}, then $k^{(0)} = k_{max} \cdot \exp(\alpha_{min})$. As already mentioned above, it is the change in α values from one reacting pair to another, and not the absolute values of α, that determine the slope of the decay curves as shown in Fig. 6. This is why it is proper to refer the distribution function $n_0(\alpha)$ in terms of a change in α, or $\Delta\alpha$, rather than in terms of the absolute values of α.

From Eqns. 5 and 6, one can calculate from the $P\text{-}700^+$ decay curves, for each given temperature, segments of the distribution functions $n_0(k)$ or $n_0(\alpha)$ corresponding to the rate constant values from $k_1 = t_1^{-1}$ to $k_2 = t_2^{-1}$, where t_1 and t_2 are the initial and the final moments of time on the decay curve. According to Eqn. 4, such a change in the rate constant corresponds to a change in α from $\alpha_1 = \ln(k^{(0)} \cdot t_1)$ up to $\alpha_2 = \ln(k^{(0)} \cdot t_2)$, or to the interval of α, $\Delta\alpha = \ln(t_2/t_1)$.

In the 160—80-K region, $k^{(0)}$ increases exponentially with increasing temperature. According to Eqn. 4, this means that for one and the same moment of time t, we observe at two different temperatures T_1 and T_2 the decay of pairs with two different α values, α_{T_1} and α_{T_2}, which are related to each other by the following equation:

$$\alpha_{T_1} - \alpha_{T_2} = \ln[k_0^{(0)} \cdot t \cdot \exp(-E'_a/RT_1)] - \ln[k_0^{(0)} \cdot t \cdot \exp(-E'_a/RT_2)]$$
$$= (E'_a/R) \cdot (1/T_2 - 1/T_1) \qquad (13)$$

From each decay curve we can reconstruct the distribution function only for the interval of $\Delta\alpha = \ln(t_2/t_1)$. But since the values of α at two different temperatures T_1 and T_2 but corresponding to the same moment of time (t_1 or t_2) are shifted, namely, by $\Delta\alpha_T = \alpha_{T_2} - \alpha_{T_1}$, it is therefore possible, from the set of decay curves obtained at various temperatures, to reconstruct the distribution function over the α values for a broader interval.

The rectangular distribution function shown in Fig. 10 was reconstructed in accordance with these ideas. First, for each temperature, parts of the function were determined as those providing the best fit between the experimental decay curves and those calculated from Eqn. 6. In the calculations for all temperatures, $\alpha_1 = \ln(k^{(0)} \cdot t_1)$ was arbitrarily assumed to be equal to zero, which corresponds to $k^{(0)} = t_1^{-1}$. Then the functions for $T = 100$, 120, 140 and 160 K were shifted along the α-axis by the appropriate intervals of $\Delta\alpha_T = (E'_a/R)\text{-}(1/80 - 1/T)$, where $E'_a = 2900$ cal/mol, and $R = 2$ cal/mol per degree. This shift reflects the actually existing relation between the $k^{(0)}$ values at various temperatures, namely, $k_{T_1}^{(0)}/k_{T_2}^{(0)} = \exp[(E'_a/R)(1/T_2 - 1/T_1)]$. Because of such a relation, it is possible to choose the value $\alpha_1 = 0$ (that is, $k^{(0)} = t_1^{-1}$) only for one temperature, say, 80 K. The values of α_1 and $k^{(0)}$ at all other temperatures are related to those values at 80 K, as $\alpha_{1,T} = \alpha_{1,80} + (E'_a/R)(1/80 - 1/T)$ and $k_T^{(0)} = t_1^{-1} \cdot \exp[(E'_a/R)(1/80 - 1/T)]$.

Fig. 6 demonstrates good agreement between the experimental kinetic curves for $P\text{-}700^+$ decay and those calculated with the help of Eqn. 6 using the distribution functions given by the solid lines in Fig. 10. When calculating the distribution function, the initial concentration, n_0, in Eqn. 6 was assumed to be the same for all temperatures. The actually observed scatter of the distribution-function levels for various temperatures appears to reflect the actual scatter of n_0 values. The condition

$$\int_{\alpha_1}^{\alpha_2} n_0(\alpha) \cdot d\alpha = \Delta n$$

(where Δn is the change of $P\text{-}700^+$ concentration during the time of the experi-

ments) was also used to find the relative positions of distribution-function levels at various temperatures.

As seen from Fig. 10, the obtained functions $n_0(\alpha)$ for all temperatures indeed correspond to a near-rectangular distribution. However, the following fact must be noted. By extrapolation of the initial linear portions of the decay curves for 80—160 K (see Fig. 6) up to the interception with the α-axis, one can find the characteristic time $t_{intercept}$ for the decay of those (P-700$^+$ ··· X$^-$) pairs which would have the largest value of α (α_{max}) and, respectively, the smallest value of the rate constant (k_{min}), assuming the distribution function $n_0(\alpha)$ had an ideal rectangular character. Then one can calculate the value of α_{max} from the relationship

$$\alpha_{max} = \ln(k^{(0)} \cdot t_{intercept}) = \ln(t_{intercept}/t_1) + (E'_a/R)(1/80 - 1/T)$$

where the last term again reflects the relation between the values of $k^{(0)}$ at 80 K (assumed to be equal to t_1^{-1}) and at other temperatures. The edges of the ideal rectangular distribution functions corresponding to the values of α_{max} obtained in this way are given in Fig. 10 by the vertical dashed lines. It is seen that these lines are shifted toward larger α values from the solid lines corresponding to the edges of the actually reconstructed near-rectangular distribution functions at 140 and 160 K.

Thus, for the interval of α-values between the solid and the dashed lines, the actual distribution functions at 140 and 160 K deviate from the rectangular one. Further experiments may be needed at even longer times (exceeding $1 \cdot 10^4$ s) to reveal the nature of these deviations. Tentatively one may ascribe them to a conformational transition starting at 140 K which perturbs the distribution function by bringing some P-700$^+$ and X$^-$ species further apart as temperature increases (also see below).

As seen from Fig. 10, the interval of $\Delta\alpha$ for which the distribution function $n_0(\alpha)$ was reconstructed here has a rather broad range of approx. 10.5. According to Eqn. 3, this corresponds to a 4.5 orders of magnitude variation in the rate constant.

As already mentioned, such a distribution may be caused either by a distribution over the values of ν, a, or over the values of r in Eqn. 9. Let us consider these possibilities in more detail.

If the distribution over k is solely due to a distribution of reacting pairs over the inter-species distance r, then $k = k^{(0)} \cdot \exp(-\alpha)$, where $\alpha = 2r/a$ and $k^{(0)} = \nu$. From these equations, the results above would yield a rectangular distribution of reacting pairs over r with $\Delta r = (a/2) \cdot \ln(t_2/t_1)$. For the typical value of $a \approx 1$ Å (for $V = 4$ eV) [38], it means a distribution $\Delta r = 5$ Å.

At temperatures below 80 K, the slope of the decay curves in Fig. 6 decreases with decreasing temperature. This phenomenon may be explained as follows: Assuming that the activation energy of 2.9 kcal/mol for the decay porcess in the 160—80-K region is associated with hindered rotation (or vibration) of some functional groups in the reacting pairs which brings P-700$^+$ and X$'^-$ into a position with a mutual orientation most favorable for tunneling. As the temperature decreases, the rotation becomes increasingly slower so that finally tunneling from the less favorable positions without any preliminary rotation or vibration becomes comparable in its rate to tunneling from the more favorable

positions which require a preliminary rotation. Thus, we have an overlap of several processes, one of which has an activation energy E'_a of 2.9 kcal/mol and the remainder has an activation energy $E''_a < E'_a$, thus resulting in a broader distribution over the values of the rate constant.

At temperatures above 160 K, the slope of the decay curves in Fig. 6 also increases with increasing temperature. This phenomenon can be explained, e.g. as a narrowing of the distribution over k values by some additional type of rotation (or vibration) with an activation energy $E_a > E'_a$ that comes into operation at higher temperatures.

Note that at still higher temperatures, when rotation (or vibration) of the reacting species in the chloroplasts can become very fast, the influence of the distribution over r, a, or ν on the $P\text{-}700^+$ decay kinetics can probably be averaged out. In this situation, the most rapid recombination of $P\text{-}700^+$ and X^- may take place as rotation or vibration rapidly places $P\text{-}700^+$ and X^- in the most favorable position for tunneling. Since displacement of centers bound to chloroplast membranes are restricted, this most favorable position may still correspond to a large distance between $P\text{-}700^+$ and X^-, so that electron tunneling may remain the only possible mechanism for recombination. But now when tunneling is characterized with a single set of r, a and ν values, the decay should follow the usual exponential kinetics. Thus, it seems that decay of $P\text{-}700^+$ in the 294—240-K region with an activation energy of 16 kcal/mol may also be an electron-tunneling process. The vlaue of the pre-exponential factor for the decay process in the 294—240-K region, $k_0 = 1 \cdot 10^{10}$ s^{-1}, which is small compared to the so-called "normal" value of $k_0 = 1 \cdot 10^{13}$ s^{-1} is also compatible with this assumption.

As seen from Fig. 9, the characteristic times, τ, for $P\text{-}700^+$ decay increase with decreasing temperature in the 180—140-K region. Just as in the case of photosynthetic bacteria [22—26], this effect can be ascribed to some conformational transition in the chloroplast membrane bringing $P\text{-}700^+$ and iron-sulfur protein closer to each other as temperature decreases. Furthermore, it is worth mentioning here that there is an important qualitative difference between the two parameters: the slope of the decay curves plotted in Fig. 6 and the characteristic time τ.

The slope as seen from Eqn. 8a reflects the span of the distribution over the value of the rate constant k, while τ is sensitive to the absolute value of k as well. Thus, in principle, the decrease of τ can be accompanied by both a decrease and an increase of the slope, depending on whether the distribution over the k values becomes broader or narrower.

Concluding remarks

Low-temperature reactions in photosynthetic bacteria and their interpretation in terms of electron tunneling have been reported for the dark reduction of the photooxidized primary donor by cytochrome c [19,20,42] and for the recombination between the oxidized primary donor and the reduced primary acceptor [21,22,41]. More recently, the decay kinetics of $P\text{-}700^+$ at low temperatures and the electron-tunneling process related to these reactions have also been reported [10,13—16].

It may be of interest to make some comparisons between the present and the earlier related works. Note first that, qualitatively, our data are in reasonable agreement with those reported in the above references. However, there is a notable difference in the quantitative analysis of the low-temperature kinetic data. In all the above works the observed decay of $P\text{-}700^+$ in the dark at low temperatures did not obey a simple exponential relationship. The decay kinetics reported earlier were either approximated with a sum of two [13] or three [14] components, plus a time-independent term which was interpreted as a contribution from the "irreversible" oxidation of the *P*-700 centers. The existence of more than one type of reduced acceptors with different reactivities toward $P\text{-}700^+$ was often postulated by other workers to account for similar kinetics [12,17]. Visser et al. [13,14] also suggested that different reactivity can be associated with different tunneling distances. We found that at high temperatures (294—240 K), the experimental decay obeys a simple exponential relationship, while at lower temperatures (220—5 K), the decay kinetics could well be described by a logarithmic or near-logarithmic relationship.

Such relationships can be explained by a continuous and broad distribution over the values of the rate constant for the tunneling recombination in various ($P\text{-}700^+ \cdots X'^-$) pairs. The distribution can arise from different environments or different mutual orientations of $P\text{-}700^+$ and X'^-, or from different distances between the two reacting species in the ($P\text{-}700^+ \cdots X'^-$) pairs. Thus our kinetic model is a natural generalization of the models proposed earlier. With this model we are now able to describe all the experimentally observed decay curves quantitatively without additional assumptions about the existence of irreversibly oxidized *P*-700 centers. Note that at short time intervals, it is very difficult to distinguish between the logarithmic function and a function representing multiple components. Thus, it seems that the low-temperature recombination kinetics previously observed by other workers could also be described by a logarithmic or near-logarithmic function.

Warden et al. [10] reported that the values of $t_{1/2}$ for $P\text{-}700^+$ decay were temperature independent below 150 K and temperature dependent at higher temperatures. An activation energy of 5.5 kcal/mol was calculated from the half-time values for the 150—270-K region [10,13]. In contrast, we observed a temperature-dependent kinetics for the whole 294—5-K region. The activation energies were estimated to be 16 and 2.9 kcal/mol for the 294—240-K and 160—80-K regions, respectively. For the 240—160-K region and for temperatures below 80 K. the activation energies cannot be determined since several different factors seem to contribute simultaneously to the temperature dependence of $P\text{-}700^+$ decay kinetics in these regions. At this time, we are inclined to attribute the discrepancy between the present and previous works to the different procedures used for the analysis of the experimental $P\text{-}700^+$ decay curves. As already demonstrated above in Fig. 9, analysis of the non-exponential kinetics in terms of $t_{1/2}$ or τ values can result in erroneous values of the activation energy.

In agreement with our data for green-plant Photosystem I, the characteristic times for the decay of the oxidized primary electron donor, $P\text{-}870^+$ (or $P\text{-}890^+$), in photosynthetic bacteria was found to increase with increasing temperature above 150 K [21,22,26,41]. This was interpreted as an indication that tunnel-

ing distance increases with increasing temperature [22] as a result of some conformational change or thermal expansion of the protein component [26].

Finally let us briefly discuss the matter of the distance between the primary reactants in the (P-700$^+$ ··· X$^-$) pairs. From the reconstructed rectangular distribution function, we have estimated the range of variation in the distances between the primary reactants to be approx. 5 Å. The actual inter-species distance may be estimated by the order of magnitude from the tunneling rates and by assuming certain values for the barrier height, the frequency factor, etc. Such estimations have been made by various workers previously for the (P-870$^+$ ··· X$^-$) system [21] in photosynthetic bacteria, and the (P-700$^+$ ··· X$^-$) system [14]. A more reliable alternative method that may be used to estimate the distance between the primary reactants in the photosynthetic reaction centers involves the dipole-dipole magnetic interaction between the two paramagnetic species, in our case, P-700$^+$ and X$^-$, as the magnetic field at a distance r from a magnetic dipole is proportional to r^{-3}. The magnetic field produced by the spin interaction of X$^-$ in the vicinity of P-700$^+$ must cause either a broadening or a splitting of the EPR line of the latter (for a detailed discussion of the dipole-dipole effects in EPR spectra see, for example, refs. 43 and 44).

During an earlier kinetic study of charge recombination in the Photosystem I reaction center, EPR spectra of light-induced P-700$^+$ and X$^-$ (reduced iron-sulfur protein) were measured simultaneously at 13 K (see Fig. 5 of ref. 15). The EPR spectrum of P-700$^+$ measured at 13 K shows a linewidth, ΔH_{pp}, of 7.5 G. It is obvious that the dipole-dipole contribution, ΔH_d, being only one of several possible contributions to the linewidth, must be smaller than 7.5 G. On the other hand, this contribution can be related to the average distance r between P-700$^+$ and X$'^-$ approximately by the relationship $\Delta H_d \lesssim g\beta/r^3$, where the g value is that for the iron-sulfur protein and β the Bohr magneton. Substituting the minimum possible g value of 1.86 for the iron-sulfur protein [37] and $0.927 \cdot 10^{-20}$ ergs/G for β into the above relationship, one obtains a lower limit of the r value of 13.2 Å.

This means that in the majority of the (P-700$^+$ ··· X$^-$) pairs the distance of electron transfer must exceed 13.2 Å. Since diffusion of P-700$^+$ and X$^-$ must be very slow at low temperatures, electron tunneling indeed seems to be the only possible mechanism for the recombination of P-700$^+$ and X$^-$.

Appendix

According to Eqn. 6,

$$n_t = \int_0^\infty n_0(\alpha) \cdot \exp[-k^{(0)} \cdot t \cdot \exp(-\alpha)]\, d\alpha \qquad \text{(A-1)}$$

For the rectangular initial distribution between the minimum and the maximum values of the distribution parameter α:

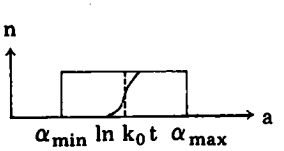

$$n_0(\alpha) = \begin{cases} n_0/(\alpha_{max} - \alpha_{min}) \text{ when } \alpha_{min} \leqslant \alpha \leqslant \alpha_{max}, \text{ and} \\ 0, \text{ when } \alpha < \alpha_{min} \text{ or } \alpha > \alpha_{max}. \end{cases}$$

The area under the rectangular profile is seen to be equal to the total initial concentration of (P-700$^+ \cdots$ X$'^-$) pairs.

For a given (P-700$^+ \cdots$ X$'^-$) pair, the characteristic decay time $t = 1/k = \exp(\alpha)/k^{(0)}$ increases sharply with increasing α. Thus, all the pairs with $\alpha < \ln(k^{(0)} \cdot t)$ must disappear by the moment t, while all the pairs with $\alpha > \ln(k^{(0)} \cdot t)$ must remain practically unreacted. One obtains for the concentration (n_t) of the remaining (P-700$^+ \cdots$ X$'^-$) pairs the following equation:

$$n_t = [n_0/(\alpha_{max} - \alpha_{min})] \cdot \int_{\ln(k^{(0)} \cdot t)}^{\alpha_{max}} \exp[-k^{(0)} \cdot t \cdot \exp(-\alpha)]\, d\alpha \qquad \text{(A-2)}$$

At α values even only slightly exceeding $\alpha = \ln(k^{(0)} \cdot t)$, the exponential term under the integral tends to unity. Thus,

$$n_t = [n_0/(\alpha_{max} - \alpha_{min})] \cdot [\alpha_{max} - \ln(k^{(0)} \cdot t)] \qquad \text{(A-3)}$$

By a more rigorous mathematical treatment one can find that approximations made when deriving this relation are valid for those t that satisfy the conditions expressed in Eqn. 7.

Relation A-3 has a simple geometric interpretation. As a result of more rapid decay of pairs with smaller α values, the profile of the distribution $n(\alpha)$ will be continuously changing with time from the side of smaller α values as shown in the above figure by a solid curve in the vicinity of $\alpha = \ln(k^{(0)} \cdot t)$. Note that the area under the initial profile to the left of this curve is equal to the concentration of pairs which disappeared by moment t while the area to the right is equal to the concentration of pairs that remained unreacted. Since the increase of the characteristic decay time with the increase of α is very sharp, it is possible to approximate these areas by the areas of the rectangles to the left and to the right of the dashed vertical line corresponding to $\alpha = \ln(k^{(0)} \cdot t)$. As seen from the above figure, the area to the right of the dashed line is equal to $[n_0/(\alpha_{max} - \alpha_{min})] \cdot [\alpha_{max} - \ln(k^{(0)} \cdot t)]$.

Acknowledgement

This work was supported in part by a National Science Foundation grant PCM-77-08455.

References

1 Calvin, M. and Sogo, P. (1957) Science 175, 499—500
2 Müller, A. and Witt, H.T. (1961) Nature 189, 944—945
3 Cost, K., Bolton, J.R. and Frenkel, A.W. (1969) Photochem. Photobiol. 10, 251—258
4 Malkin, R. and Bearden, A.J. (1972) Proc. Natl. Acad. Sci. U.S. 68, 16—19
5 Yang, C.S. and Blumberg, W.E. (1972) Biochem. Biophys. Res. Commun. 46, 422—428
6 Vredenberg, W.J. and Duysens, L.N.M. (1965) Biochim. Biophys. Acta 94, 355—370
7 Mayne, B.C. and Rubinstein, D. (1966) Nature 210, 734—745
8 Vernon, L.P., Ke, B. and Shaw, E.R. (1972) Biochemistry 6, 2210—2220
9 Witt, K. (1973) FEBS Lett. 39, 112—115
10 Warden, Jr., J.T., Mohanty, P. and Bolton, J.R. (1974) Biochem. Biophys. Res. Commun. 59, 872—878
11 Warden, Jr. J.T. (1972) Dissertation, University of Minnesota
12 Lozier, R.H. and Butler, W.L. (1974) Biochim. Biophys. Acta 333, 465—480

15 Ke, B., Sugahara, K., Shaw, E.R., Hansen, R.E., Hamilton, W.D. and Beinert, H. (1974) Biochim. Biophys. Acta 368, 401—408
16 Ke, B., Sugahara, K. and Sahu, S. (1976) Biochim. Biophys. Acta 449, 84—89
17 Shuvalov, V.A., Klimov, V.V. and Krasnovskii, A.A. (1976) Mol. Biol. 10, 326—339
18 Bearden, A.J. and Malkin, R. (1974) Fed. Proc. 33, Abstr. 378
19 DeVault, D. and Chance, B. (1966) Biophys. J. 6, 825—847
20 DeVault, D., Parkes, J.H. and Chance, B. (1967) Nature 215, 642—644
21 McElroy, J.D., Mauzerall, D.C. and Feher, G. (1974) Biochim. Biophys. Acta 333, 261—277
22 Hsi, E.S.P. and Bolton, J.R. (1974) Biochim. Biophys. Acta 347, 126—133
23 Grigorov, L.N. and Chernavskii, D.S. (1972) Biofizika 17, 195—202
24 Hopfield, J.J. (1974) Proc. Natl. Acad. Sci. U.S. 71, 3640—3644
25 Jortner, J. (1976) J. Chem. Phys. 64, 4860—4867
26 Hales, B.J. (1976) Biophys. J. 16, 471—480
27 Vernon, L.P. and Shaw, E.R. (1971) Methods Enzymol. 23, 277—289
28 Ke, B. (1972) Methods Enzymol. 24, 25—53
29 Ke, B., Sahu, S., Shaw, E.R. and Beinert, H. (1974) Biochim. Biophys. Acta 347, 36—48
30 Ke, B. (1975) in Proceedings at the 3rd International Congress in Photosynthesis (Avron, M., ed.), Vol. 1, pp. 373—382, Elsevier, Amsterdam
31 Ke, B., Dolan, E., Sugahara, K., Hawkridge, F., Demeter, S. and Shaw, E.R. (1977) Plant Cell Physiol., special issue, 187—199
32 Demeter, S. and Ke, B. (1977) Biochim. Biophys. Acta 462, 770—774
33 McIntosh, A.R., Chu, M. and Bolton, J.R. (1975) Biochim. Biophys. Acta 376, 308—314
34 Evans, M.C.W., Sirha, C.K., Bolton, J.R. and Cammack, R. (1975) Nature 256, 668—670
35 Malkin, R. and Bearden, A.J. (1971) Proc. Natl. Acad. Sci. U.S. 68, 16—19
36 Evans, M.C.W., Telfer, A. and Lord, A.V. (1972) Biochim. Biophys. Acta 267, 530—537
37 Ke, B., Hansen, R.E. and Beinert, H. (1973) Proc. Natl. Acad. Sci. U.S. 40, 2941—2945
38 Zamaraev, K.I. and Khairutdinov, R.F. (1974) Chem. Phys. 4, 181—194
39 Gamow, G. (1928) Z. Phys. 51, 204—212
40 Alexandrov, J.V., Khairutdinov, R.F. and Zamaraev, K.I. (1978) Chem. Phys., in the press
41 Loach, P., Kung, M. and Hales, B.J. (1975) Ann. N.Y. Acad. Sci. 224, 297
42 Kihara, T. and Chance, B. (1969) Biochim. Biophys. Acta 189, 116—124
43 Feher, G. (1970) Electron Paramagnetic Resonance with Applications to Selected Problems in Biology, Gordon and Breach, New York
44 Wyard, S.J. (1965) Proc. Phys. Soc. 65, 587—593